Simulation of Structural and Fluid Flow Response in Engineering Practice

KLAUS-JÜRGEN BATHE
Massachusetts Institute of Technology, Cambridge, MA 02139

Abstract: Some current state-of-the art approaches and procedures to model the response of structures, fluids, and fluid flows with structural interactions are presented. The emphasis is on general and reliable techniques that can be used in engineering practice. As illustration, various complex analyses are briefly discussed. The objective is to show that, in engineering practice, very complex analyses can already be performed with confidence, and to briefly point toward further important research and development tasks.

1. INTRODUCTION

The simulation of the response of structural and fluid flow systems using numerical methods is now firmly established in engineering practice. It is common that a design is analyzed for anticipated loads to ensure a safe system that also can be built economically. Indeed, the competitive environment to bring improved and more economical structures and mechanical components speedily to market makes the use of sophisticated analysis tools imperative.

In structural analysis, the most widely used numerical technique is the finite element method. While at present, fluid systems are still largely solved using finite difference and control volume methods, finite element techniques show great promise here too and are used to an increasing extent (Zienkiewicz and Taylor, 1989/1990; Bathe, 1995).

Figure 1 shows schematically the process of analysis of a structure or fluid system. The first step in the analysis consists of defining the geometry, material data, and boundary conditions. The geometry may be created by the analyst or be imported from the data of a CAD program (see Section 3.7). Once this basic information is available, in a second step, the analyst defines the mathematical model to be solved. Here the analyst may confront the analysis of a structural system, fluid system, or fluid-structure system, and must define the details of the

---

Acknowledgement: I would like to thank E. Bøyum of Kværner Energy, Oslo, Norway, P. Reimers of Iwis, Berlin, Germany, J. MacIntyre of The California State Department of Transportation, Sacramento, CA, and A. Krimotat of SC Solutions, Mountain View, CA, for providing some figures presented in this article.
Communicated by S. N. Atluri, 09/29/95.

Computer Modeling and Simulation in Engineering 1: 47-77, 1996

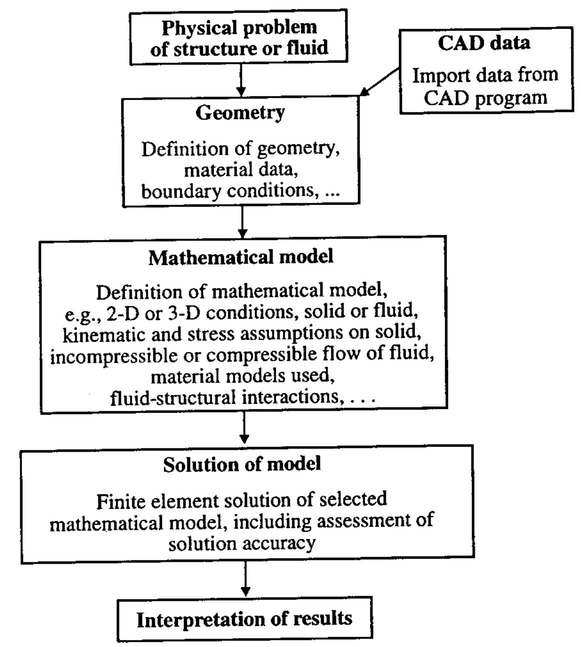

Figure 1. Process of analysis.

mathematical model. This step is the most crucial one in the complete analysis process and involves the idealization of the geometry, kinematic behavior, representation of the loads, boundary conditions, material behavior, the decision on whether a steady state or transient solution needs to be obtained, and so on. The solution of the mathematical model is then performed using the available numerical methods and this step should include an assessment of the solution error, that is, an assessment of how accurately the exact solution of the mathematical model has been approximated. Finally, the solution results are interpreted, which may lead to the need to refine the mathematical model and perform further finite element solutions.

The objective in this article is to present some current state-of-the-art approaches and procedures of analysis, and point toward important further research and development tasks. We consider structural and fluid systems and the interaction between structures and fluids. In the following sections of the article, we first briefly state the basic governing equations that are solved in various mathematical models, and then review the current state of finite element solution methods. We emphasize that specific care must be exercised to use reliable and cost-effective mathematical models and, for solution, only reliable finite element procedures. Indeed, certain finite element techniques that have been widely published should not be employed in practical analysis. We illustrate our observations with some industrial analysis examples. Finally, we conclude by focusing on some important outstanding issues in the field.

2. MATHEMATICAL MODELS AND ISSUES

We start by reviewing briefly the general governing continuum mechanics equations of the mathematical models that we consider, and then present some important issues regarding the appropriate choice of model.

2.1. Structural Response Equations

The basic differential equations modeling a structural response in small and large deformations and with general nonlinear material characteristics have been extensively considered (Bathe, 1995). Assuming a stationary Cartesian reference frame (x_i, i = 1, 2, 3), index notation, and the usual summation convention, the equations are in Lagrangian form

Momentum

$$\rho \frac{d^2 u_i}{dt^2} = \tau_{ij,j} + f_i^B \tag{1}$$

Constitutive

$$\tau_{ij} = \tau_{ij} \text{ (current strains, history, time, . . .)} \tag{2}$$

Compatibility

$$\text{Continuous displacements } u_i \text{ and } u_i = u_i^{S_u} \text{ on the surface } S_u. \tag{3}$$

Also, the force boundary conditions are

$$\tau_{ij} n_j = f_i^{S_f} \text{ on the surface } S_f. \tag{4}$$

In Equations (1) to (4), we have, τ_{ij}, the components of the Cauchy stress tensor; u_i, the components of the displacement vector; ρ, the mass density; f_i^B, the components of the externally applied body force vector; n_i, the components of the unit normal vector to the body surface; $u_i^{S_u}$ and $f_i^{S_f}$, the components of the imposed displacements and tractions; $S_u \cup S_f = S$, (the complete surface area), and $S_u \cap S_f = 0$.

Equations (1) to (4) must be satisfied at all times during the response. To consider a specific time in the solution, we use a left superscript t on the variable. The solution of these governing equations is, in many cases, effectively obtained using the total Lagrangian formulation (Bathe, 1995), which in variational form is, at time t,

$$\int_{^0V} {}^t_0 S_{ij}\, \delta\, {}^t_0\varepsilon_{ij}\, d\,^0V = {}^t\Re, \tag{5}$$

where we have ${}^t_0S_{ij}$ and ${}^t_0\varepsilon_{ij}$, respectively, the components of the 2nd Piola-Kirchhoff stress and Green-Lagrange strain tensors; δ means "variation in" and all quantities are referred to the original volume ${}^0V$ of the body. The relation in Equation (5) is the celebrated principle of virtual work (or "weak form" of the Equations [1] to [4]). The internal virtual work is given on the left-hand side and the external virtual work is given in ${}^t\Re$ and includes all effects of applied body, inertia and surface forces. This equation is valid for the 1-, 2- and 3-dimensional response of solids and, with appropriate constraints and assumptions on the kinematics and stresses, for the structural response of beams, plates, and shells. Transitional regions between solid and structural regions can also be modeled (Bathe, 1995). Hence Equation (5) represents a very general basis for finite element discretizations of general structures and solids.

2.2. Incompressible Fluid Flow Equations

In many practical fluid flow situations, the fluid flows approximately as an incompressible medium. In these cases, the mathematical model assuming total incompressibility is correctly employed, and we have the following governing Navier-Stokes equations.
Momentum

$$\rho\left(\frac{\partial v_i}{\partial t} + v_{i,j}v_j\right) = \tau_{ij,j} + f_i^B \tag{6}$$

Constitutive

$$\tau_{ij} = -p\delta_{ij} + 2\mu e_{ij} \tag{7}$$

Continuity / conservation of mass

$$v_{i,i} = 0 \tag{8}$$

Energy

$$\rho c_p\left(\frac{\partial\theta}{\partial t} + \theta_{,i}v_i\right) = (k\theta_{,i})_{,i} = q^B + 2\mu e_{ij}\, e_{ij}\,, \tag{9}$$

where we have, v_i, velocity of fluid flow in direction x_i; ρ, mass density, constant; τ_{ij}, components of stress tensor; f_i^B, components of body force vector; p, pressure; δ_{ij}, Kronecker delta; μ, fluid viscosity, velocity- and temperature-dependent; e_{ij}, components of velocity strain tensor $= \frac{1}{2}(v_{i,j} + v_{j,i})$; c_p, specific heat at constant pressure, temperature-dependent; θ, temperature; k, thermal conductivity, temperature-dependent; q^B, rate of heat generated per unit volume, temperature-dependent.

The boundary conditions corresponding to Equations (6) to (9) are:

- prescribed fluid velocities, $v_i^{S_v}$ on the surface S_v

$$v_i\Big|_{S_v} = v_i^{S_v}\,; \tag{10}$$

- prescribed tractions, $f_i^{S_f}$, on the surface S_f

$$\tau_{ij}n_j\Big|_{S_f} = f_i^{S_f}\,; \tag{11}$$

- prescribed temperature, θ^{S_θ}, on the surface S_θ

$$\theta\Big|_{S_\theta} = \theta^{S_\theta}\,; \tag{12}$$

- prescribed heat flux, q^{S_q}, into the surface S_q

$$k\frac{\partial\theta}{\partial n}\Big|_{S_q} = q^{S_q}\,. \tag{13}$$

We note that $S_v \cup S_f = S, S_v \cap S_f = 0$ and $S_\theta \cup S_q = S, S_\theta \cap S_q = 0$, where S is the total surface area of the fluid body. With these equations, we solve interior and exterior flow conditions, where for exterior flow conditions, the domain of analysis must be chosen sufficiently large.

The heat flow input in Equation (13) comprises the effect of actually applied distributed heat flow and the effect of convection and radiation heat transfer.

In addition, we have for a free surface $S(x_i, t)$ the boundary conditions

$$\frac{\partial S}{\partial t} + S_{,j}v_j = 0 \tag{14}$$

and

$$\tau_{ij}n_j = \left(p_0 + \sigma\left(\frac{1}{R_1} + \frac{1}{R_2}\right)\right)n_i\,, \tag{15}$$

where σ is the surface tension coefficient, p_0 is the ambient pressure, and R_1, R_2 are the radii of curvatures of the free surface.

The above fluid flow equations correspond to laminar flow. Turbulence conditions can be represented using various turbulence models, including the k-ε model.

Equations (6) to (9) are in conservative form

$$\frac{\partial \boldsymbol{U}}{\partial t} + \nabla \bullet (\mathbf{F} - \mathbf{G}) = \mathbf{S}\,, \tag{16}$$

with

$$\mathbf{U} = \begin{bmatrix} 0 \\ \rho\mathbf{v} \\ \rho E \end{bmatrix}, \tag{17}$$

$$\mathbf{F} = \begin{bmatrix} \rho\mathbf{v} \\ \rho\mathbf{vv} \\ \rho\mathbf{v}E - \boldsymbol{\tau}\bullet\mathbf{v} \end{bmatrix}, \tag{18}$$

$$\mathbf{G} = \begin{bmatrix} \mathbf{0} \\ \tau \\ -\mathbf{q} \end{bmatrix}, \tag{19}$$

$$\mathbf{S} = \begin{bmatrix} 0 \\ \mathbf{f}^B \\ \mathbf{f}^B\bullet\mathbf{v} + q^B \end{bmatrix}, \tag{20}$$

where we have, E, specific energy $= \frac{1}{2}\mathbf{v}\bullet\mathbf{v} + e$; e, internal energy; $\mathbf{q}$, heat flux $= -k\nabla\theta$.

In this mathematical model, we assume that de $= c_v d\theta$ where c_v is the specific heat at constant volume and $c_v = c_p$.

The variational form of the above Navier-Stokes equations is

$$\int_V \left(w_i \left(\frac{\partial \boldsymbol{U}}{\partial t} + \nabla \bullet \mathbf{F} - \mathbf{S} \right) + \nabla w_i \bullet \mathbf{G} \right) dV = \int_S w_i \mathbf{G} \bullet \mathbf{n}\, dS, \tag{21}$$

where w_i represents the *ith* Galerkin trial function. We use this representation to obtain the governing finite element equations.

2.3. *Compressible Fluid Flow Equations*

When the Mach number of the fluid velocities is larger than approximately 0.2, the compressibility effects of the fluid must be included, and we have the following governing Navier-Stokes equations.
Momentum

$$\rho\left(\frac{\partial \mathrm{v}_i}{\partial t} + \mathrm{v}_{i,j}\mathrm{v}_j\right) = \tau_{ij,j} + f_i^B \tag{22}$$

Constitutive

$$\tau_{ij} = -(p - \lambda \mathrm{v}_{k,k})\delta_{ij} + 2\mu e_{ij} \tag{23}$$

Continuity / conservation of mass

$$\frac{\partial \rho}{\partial t} + (\rho \mathrm{v}_i)_{,i} = 0 \tag{24}$$

Energy

$$\frac{\partial(\rho E)}{\partial t} + (\rho \mathrm{v}_i E - \mathrm{v}_j \tau_{ji} + q_i)_{,i} = f_i^B \mathrm{v}_i + q^B, \tag{25}$$

where now ρ is of course not constant, and λ is the second viscosity factor (in Stokes' hypothesis $\lambda = -\frac{2}{3}\mu$).

The conservative form of these equations is still

$$\frac{\partial \boldsymbol{U}}{\partial t} + \nabla \bullet (\mathbf{F} - \mathbf{G}) = \mathbf{S}, \tag{26}$$

but, for the compressible flow conditions,

$$\mathbf{U} = \begin{bmatrix} \rho \\ \rho\mathbf{v} \\ \rho E \end{bmatrix}. \tag{27}$$

The finite element solution is again obtained using Equation (26) in variational form, see Equation (21). Comparing the governing equations of compressible fluid flow with those of the incompressible flow, we notice the commonalities, but for Equation (26) we need to use the equations of state

$$\rho = \rho(p, \theta) \tag{28}$$

$$e = e(p, \theta), \tag{29}$$

which for a perfect gas give $\rho = p/((c_p - c_v)\theta)$ and $e = c_v\theta$. However, a more general description, as implied in Equations (28) and (29), can be used (see the ADINA system users manuals, 1995).

The basic solution variables in the incompressible fluid flow equations are the unknown primitive variables, i.e., the velocities, pressure, and temperature. We also employ the same variables for the visualization of compressible fluid flows, but use the conservative variables ρ, $\rho \mathrm{v}_i$ and ρE for the solution. The boundary conditions for compressible flows can be specified using either the primitive or conservative variables and various different conditions can be imposed depending on the type of flow. Of course, viscous effects can be neglected in the above equations, and then the Euler equations are solved.

2.4. Arbitrary Lagrangian-Eulerian Formulation

For the analysis of fluid flows with structural interactions, it is effective to use an arbitrary Lagrangian-Eulerian (ALE) formulation to describe the fluid flow. This formulation can be directly coupled with a Lagrangian formulation for the structural response.

The essence of the ALE formulation is that the spatial position for the evaluation of the total time derivative of the variables of a fluid particle is not fixed in space, but is allowed to move. The motion is selected in the solution of the equations but does not necessarily correspond to the particle motion (which would be the case in a pure Lagrangian formulation).

Let $\mathbf{v}_m$ be the velocity vector of the spatial position used for the time derivative of a variable, then the total time derivative of that variable is given by

$$\frac{d(\cdot)}{dt} = \frac{\delta(\cdot)}{\delta t} + (\mathbf{v} - \mathbf{v}_m) \bullet \nabla(\cdot)\,, \tag{30}$$

where $\delta(\cdot)/\delta t$ is the time derivative with respect to the spatial position. We use equation (30) to express the total time derivatives in equations (16) and (26), and judiciously prescribe the velocity vector $\mathbf{v}_m$ in the finite element solution process.

2.5. Choice of Mathematical Model

The idealization of the physical problem to an effective mathematical model is perhaps the most difficult aspect of an engineering analysis, and it is certainly the most important step in the analysis. It is clear that a finite element solution will solve *only* the selected mathematical model, and we cannot expect from a finite element solution any more information in the prediction of a physical phenomenon than what is contained in the mathematical model.

The actual mathematical model chosen for the analysis must depend on the questions asked. The model is reliable if it is known that the answers to these questions will be obtained within an allowable error, and the model is most effective if the least amount of effort is expended to obtain the answers. Here, we refer to the error in the specific answers between the *exact* solution of the chosen mathematical model and the *exact* solution of a "very-comprehensive" mathematical model, which models nature very comprehensively in all details (Bathe, Lee, and Bucalem, 1990). The error of the numerical solution in solving the chosen mathematical model needs to be assessed also and we refer to this aspect in Section 3.8.

It is important to note here, too, that by seemingly increasing the complexity of the mathematical model, in fact the solution effort may be reduced and more accurate answers may be obtained (see Bathe, 1995). The choice of an appropriate mathematical model is therefore crucial and will largely determine the effort that is needed to perform the analysis.

3. FINITE ELEMENT DISCRETIZATION—SOME SPECIAL ISSUES

The finite element solution of the continuum mechanics equations presented in the previous section has been discussed previously (see, for example, Zienkiewicz and Taylor, 1989/1990; Bathe, 1995; Bathe, Zhang, and Wang, 1995). However, there are some special difficulties that only recently have been solved satisfactorily and some difficulties are still prominent. We address some of these topics in this section.

3.1. Solution of Incompressible Response

Effective procedures for the practical analysis of almost or totally incompressible solid and fluid models have only recently been developed based on the use of mixed methods. An effective procedure for the analysis of solids uses the principle of virtual work in Equation (5), but amended such that displacements and pressure are the primary variables. This approach corresponds to an application of the Hu-Washizu variational principle or Hellinger-Reissner principle (Bathe, 1995).

In the analysis of fluids, the formulations already contain pressure as a primary variable, see Equations (7) and (23), and, hence, Equation (21) can directly be discretized.

However, in each case, the key to the success of the finite element discretization is that the *specific element interpolations* used must satisfy the inf-sup condition (Brezzi and Bathe, 1990; Bathe, 1995).

$$\inf_{q_h \in Q_h} \; \sup_{\mathbf{v}_h \in V_h} \; \frac{\int_{Vol} q_h \operatorname{div} \mathbf{v}_h \, dVol}{\| q_h \|_0 \, \| \mathbf{v}_h \|_1} \geq c > 0\,,$$

where Q_h and V_h are the selected pressure and displacement (or velocity) spaces, respectively, and c is a constant independent of the material properties and the generic element size, h. If a discretization satisfies this condition, it is stable and optimal in error for the chosen element interpolations. In practice, for incompressible analysis, we should only use element formulations that satisfy the inf-sup condition.

We may remark here that frequently reduced integration schemes are still employed to analyze an incompressible medium. In some cases, adequate results may be obtained, but these methods lack the robustness and generality of a properly formulated mixed method, and may indeed lead to erroneous results (Bathe, 1995).

3.2. Large Strain Analysis of Solids

The large deformation analysis of solids can be of great importance to simulate a manufacturing process (e.g., in metal forming), or to investigate the general performance of a certain part (e.g., the wear of a motor-car tire) or to analyze the collapse response of a structure. For these analyses, it is important to use an effective Lagrangian formulation that does not restrict the magnitude of the strains. Also, since at large strains, material behaviors are frequently acting in almost incompressible conditions, the considerations given in the preceding section are applicable. For the analysis of large elastic strain conditions, a total Lagrangian formulation based on models of strain energy densities is effective (Sussman and Bathe, 1987; Bathe, 1995), whereas for the analysis of situations involving large inelastic strains, a Lagrangian formulation based on the Hencky strain measure is efficient (Bathe, 1995; Gabriel and Bathe, 1995). In such applications, frequently contact conditions must be included as well and the constraint function method represents an attractive approach (Bathe, 1995).

3.3. *Analysis of Plates and Shells*

The development of solution methods for general plate and shell structures has presented formidable difficulties, but during the recent years, general and effective finite element discretization techniques have been proposed. Specifically, the procedure based on mixed interpolation of tensorial components (MITC) has resulted in effective elements (the MITC elements) (Bathe and Dvorkin, 1986; Bathe, Bucalem, and Brezzi, 1990; Bucalem and Bathe, 1993; Bathe, 1995). The essence of the formulation is to use different interpolations for the various components of the strain tensor and tie these to the usual displacement interpolations used with Equation (5).

The evaluation of these elements is obtained using full numerical integration. Of course, the elements do not contain any spurious zero energy modes typically found in elements based on reduced integration. In practical analysis, elements with spurious zero energy modes should not be employed, because their use may lead to erroneous solutions.

3.4. *High Reynolds and Peclet Number Flows*

During the recent years remarkable advances have taken place in the development of finite element methods for fluid flow analysis (Franca, Frey and Hughes, 1992; Bathe, 1995; Bathe, Zhang, and Wang, 1995). At present, the state of the art regarding fluid flow analysis allows the solution of very complex flows in intricate geometries. For this reason, finite element fluid flow analyses including heat transfer are conducted to an increasing extent in engineering practice. In our approach, we have embedded control volume type procedures into the finite element discretization scheme such that for low Reynolds number flows, we satisfy the inf-sup condition, and for high Reynolds number flows, we use upwinding procedures of control volume methods (Patankar, 1980; Bathe, Zhang, and Wang, 1995). This approach is effective for the mathematical models of incompressible *and* compressible fluid flows because overall, even when we consider high-speed flow, regions of low Mach number flow will probably be present and therefore the discretizations should satisfy the inf-sup condition.

3.5. *Fluid-Structure Interactions*

An analysis area that has attracted interest to an increasing extent during the recent years is the analysis of fluid-structure interactions. Here we may distinguish at least three application areas, namely, the analysis of fluid flows in porous media (e.g., consolidation problems), the analysis of acoustic fluid-structure interactions, and the solution of fluid flows governed by the full Navier-Stokes or Euler equations with structural interactions. Significant research and developments have taken place in each of these application areas. For the analysis of porous media, efficient computational procedures are now available (Lewis and Schrefler, 1987; Zienkiewicz and Taylor, 1989/1990) and for the solution of acoustic fluid-structure interactions, in addition to potential-based procedures, primitive variable-based procedures can now also be used with confidence (Bathe, Nitikitpaiboon, and Wang, 1995; Wang and Bathe, 1995). In many practical situations, analyses in these two areas can at present be conducted in a routine manner. Also, solutions of the full Navier-Stokes equations fully coupled to structural response in complex practical geometries while frequently still a formidable task, can now be obtained (Bathe, Zhang, and Wang, 1995). In the ADINA system, we use an arbitrary Lagrangian-Eulerian formulation for the fluid, and a Lagrangian formulation for the solid or structure. An important aspect of the solution is that different mesh densities can be used to discretize the structure and the fluid. Of course, the fluid representation usually requires a much finer mesh than the representation of the structure (for which also higher-order elements than for the fluid may be used).

3.6. *Iterative Solution of Governing Equations*

An important ingredient in the finite element solution of the mathematical model is the solution of the governing algebraic equations

$$\mathbf{A}\mathbf{x} = \mathbf{b}, \tag{31}$$

where $\mathbf{A}$ is the coefficient matrix, $\mathbf{x}$ is the solution vector and $\mathbf{b}$ is the forcing vector. The coefficient matrix $\mathbf{A}$ is usually symmetric in structural analysis and nonsymmetric in fluid flow solutions. Using a direct solution scheme (based on some variant of Gauss elimination), the solution time and required hardware resources increase approximately in proportion to N^2 and $N^{3/2}$, where N is the size of the matrix. Hence, practical limitations for the solution of large systems are quickly reached. For this reason, much emphasis has been placed on the development of iterative methods, and during recent years significant advances have been made (Bathe, 1995).

Effective iterative schemes for finite element analysis are based on the conjugate gradient technique and the generalized minimal residual (GMRes) method. However, the key to obtaining an effective method is the preconditioner; various schemes have been proposed. An effective preconditioner can reduce drastically the number of iterations required for convergence, such that the solution time may be significantly less than in a direct solution. Also, large savings in the storage requirements can be obtained (Bathe, Walczak, and Zhang, 1993).

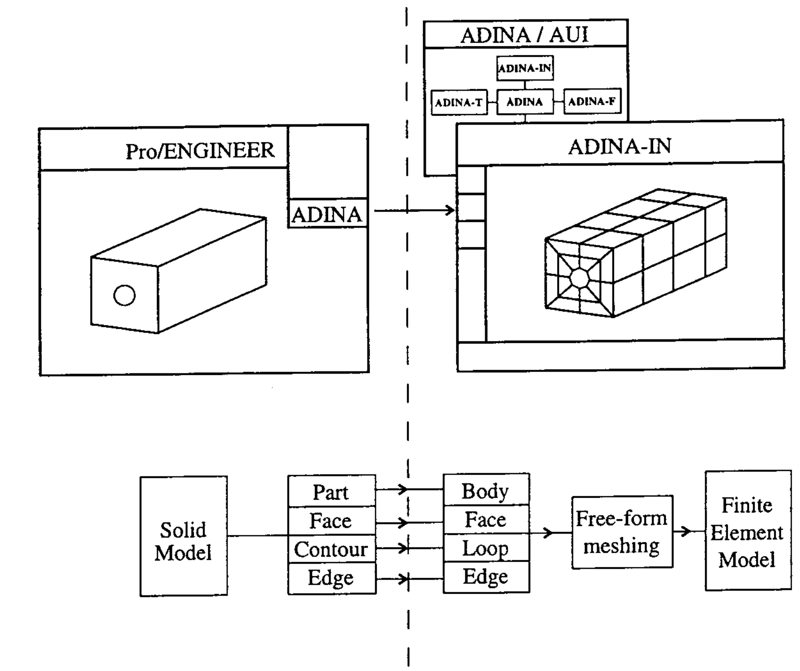

Figure 2. The ADINA system used with Pro/Engineer.

We have found that effective preconditioners can be based on incomplete factorizations of the coefficient matrices, and use these for our conjugate gradient and GMRes implementations. These procedures have shown large savings in solution times and storage (see Section 4.1).

3.7. Finite Element Analysis in Computer-Aided Design (CAD)

A large application field of finite element analysis is the area of CAD. Here the process of analysis is only one step in the complete design cycle, but an important step. Once the geometry has been established and the material properties and loads have been defined, the design engineer may want to perform a finite element analysis with software that proceeds in a quite automatic manner with the complete analysis. Engineering designers are not necessarily very knowledgeable analysts and therefore require software tools that automatically (or at least semiautomatically) carry out the envisaged analysis. Figure 2 shows how the coupling of the finite element system ADINA with the CAD program Pro/Engineer has been accomplished.

Considering linear static analysis, such automatic procedures are now available to a high degree, but dynamic and nonlinear analyses are much more difficult. These still require considerable knowledge on the part of the analyst and some important decision making regarding the finite element mesh and solution procedures to be used (see Bathe, 1995).

Two ingredients in the automatic analysis are the automatic meshing and the calculation of error measures for the finite element solution. The mesh must be constructed automatically on the geometry made available by the CAD software.

Various basic schemes are available for this task (e.g., the advancing front method and the paving/plastering scheme [George, 1991; Blacker and Meyers, 1993]), but there is still need to develop effective mesh generation schemes for three-dimensional brick element discretizations of complex geometries.

The error measures can be obtained as briefly mentioned in the following section. With these error measures, it is then possible to refine (and sometimes derefine) various parts of the mesh in steps until a sufficiently accurate numerical solution of the mathematical model used has been obtained.

Of course, in principle, the same automatic process could also be pursued in dynamic and nonlinear analyses, but, as already mentioned above, here some steering by the analyst is required to ensure that the goals of solution are achieved without an excessive amount of computations.

3.8. Error Measures

With the finite element solution, we solve numerically the chosen mathematical model (see Section 2.5). Hence, we must expect numerical errors. These errors can be measured by identifying how far the numerical solution satisfies the conditions of an exact solution; for example, in structural analysis compatibility, the stress-strain law, and differential equilibrium. Assuming a linear static analysis and a displacement-based finite element discretization, we satisfy the compatibility conditions and the stress-strain law exactly, and the error lies in not satisfying to a sufficient accuracy the differential stress equilibrium (in addition, there are usually small errors in representing the geometry, using numerical integration, due to round-off in the solution of the equations, and so on [see Bathe, 1995]). Using parabolic elements, which are widely employed, the error in the stress equilibrium can be measured by the discontinuities in the unsmoothed stress bands (see Sussman and Bathe, 1986; Lee and Bathe, 1994; Bathe, 1995). Large discontinuities indicate that the mesh is too coarse, and for an accurate solution of the mathematical model, the mesh should be refined.

A significant amount of research has been focused on identifying accurate error measures (Zienkiewicz and Zhu, 1987; Zienkiewicz and Taylor, 1989/1990; Lee and Bathe, 1994; Bathe, 1995). In almost all cases, error measures based on energy norms have been proposed. However, it is more valuable to directly obtain (and "see") the error in *stresses* in the regions of interest, and the isoband procedure referred to above displays this error.

Using the appropriate variables this isoband procedure can also be applied in fluid flow analysis.

4. APPLICATION EXAMPLES

The following applications of finite element procedures are presented to briefly illustrate the above discussion. The results indicate the kind of simulations that can be performed at the present time and they will also point toward further valuable developments in the field that we then address briefly in Section 5.

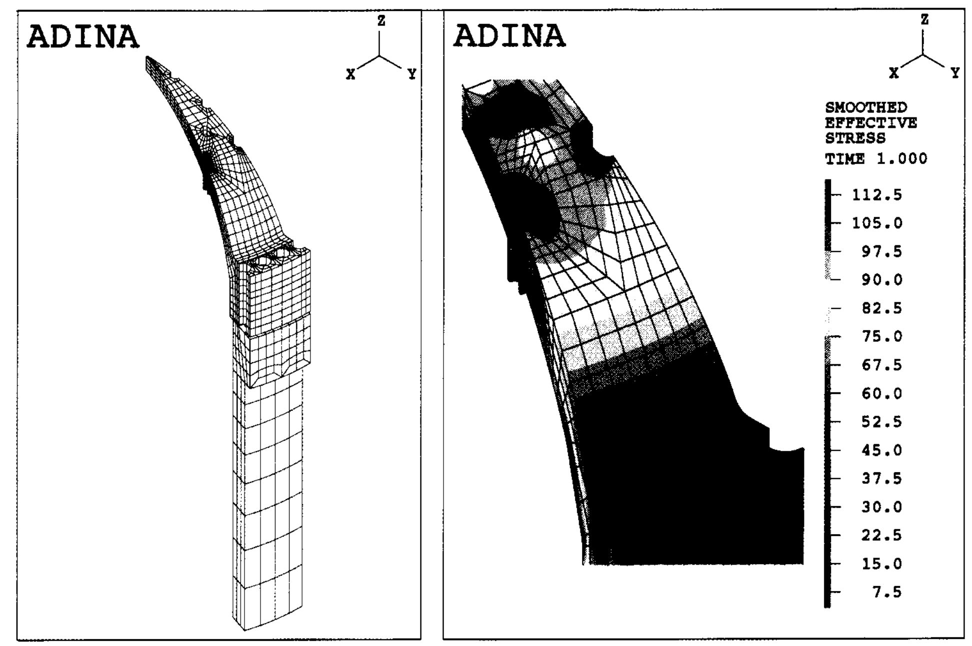

Figure 3. Model of cover of a reactor pressure vessel.

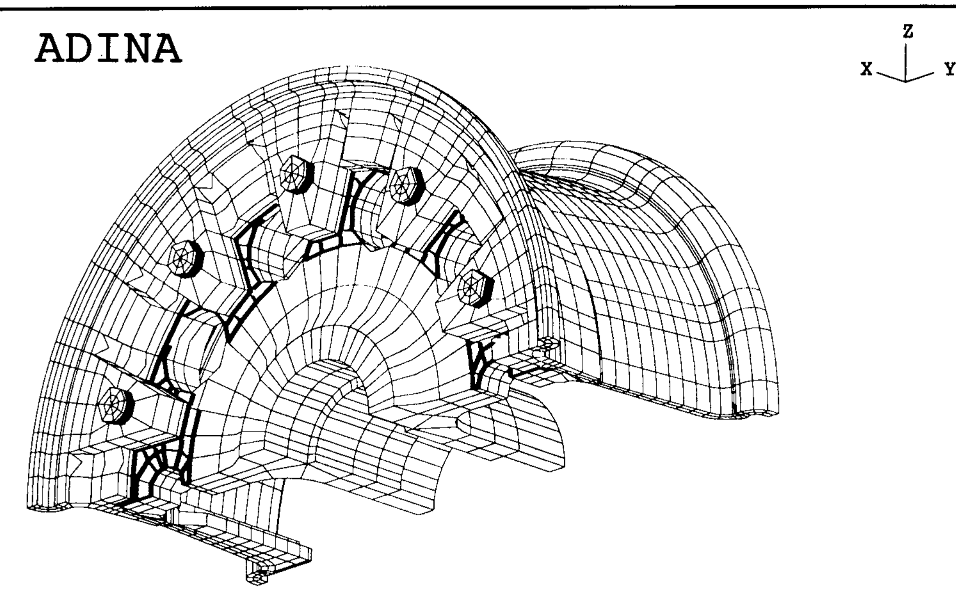

Figure 4. Model of F16 jet wheel.

4.1. Use of Iterative Solver

As pointed out in Section 3.6, the use of an iterative solver can significantly reduce the required solution time and hardware resources. The solver can be of particular benefit if large finite element systems are to be solved on engineering workstations or PCs.

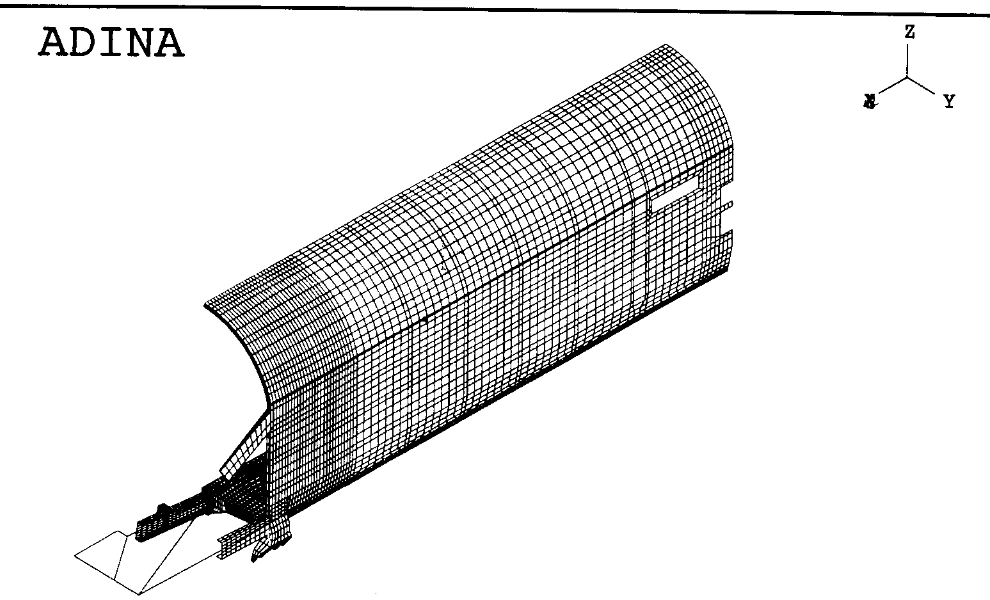

Figure 5. Model of railroad car.

Table I. Analysis of cover of a reactor pressure vessel.

	Direct Solver	*Iterative Solver*	*Ratio*
CPU time	6,137 sec (~1.75 hr)	1,034 sec (~0.25 hr)	5.94
Storage requirements (words)	191,419,272	12,863,211	14.9

NOTE: Number of equations: 58,707; Elements used: 3-D SOLID, 20-node elements; Type of analysis: linear static; Number of iterations: 496; Computer: IBM RISC 6000/550 workstation.

Table II. Three-dimensional contact analysis of an F-16 jet wheel.

	Direct Solver	*Iterative Solver*	*Ratio*
CPU time	15,923 sec (~4.5 hr)	13,726 sec (~3.75 hr)	1.16
Elapsed time	49,987 sec (~14 hr)	15,131 sec (~4.25 hr)	3.30
Storage requirements (words)	119,210,734	9,523,056	12.5

NOTE: Number of equations: 51,159; Elements used: 3-D SOLID, 20-node elements; Type of analysis: elastic with 3-D contact; Number of Newton-Raphson iterations: 8; Mean number of iterations per equation solution: 759; Computer: DEC Alpha AXP 3000 workstation.

In fluid flow simulations, it is quite necessary and common to use an iterative solver for any practical three-dimensional analysis. However, in structural analysis, direct solution schemes are commonly used and iterative procedures have only recently been applied with major advantages. The example solutions summarized in Figures 3 to 5 and Tables I to III give some typical comparisons between direct

Table III. Analysis of a railroad car.

	Direct Solver	*Iterative Solver*	*Ratio*
CPU time	4,578 sec (~1.25 hr)	4,743 sec (~1.25 hr)	.97
Storage requirements (words)	212,472,244	7,779,693	27.3

NOTE: Number of equations: 90,825; Elements used: four-node SHELL MITC4 elements, BEAM elements; Type of analysis: linear static; Number of iterations: 3,779; Computer: IBM RISC 6000/550 workstation.

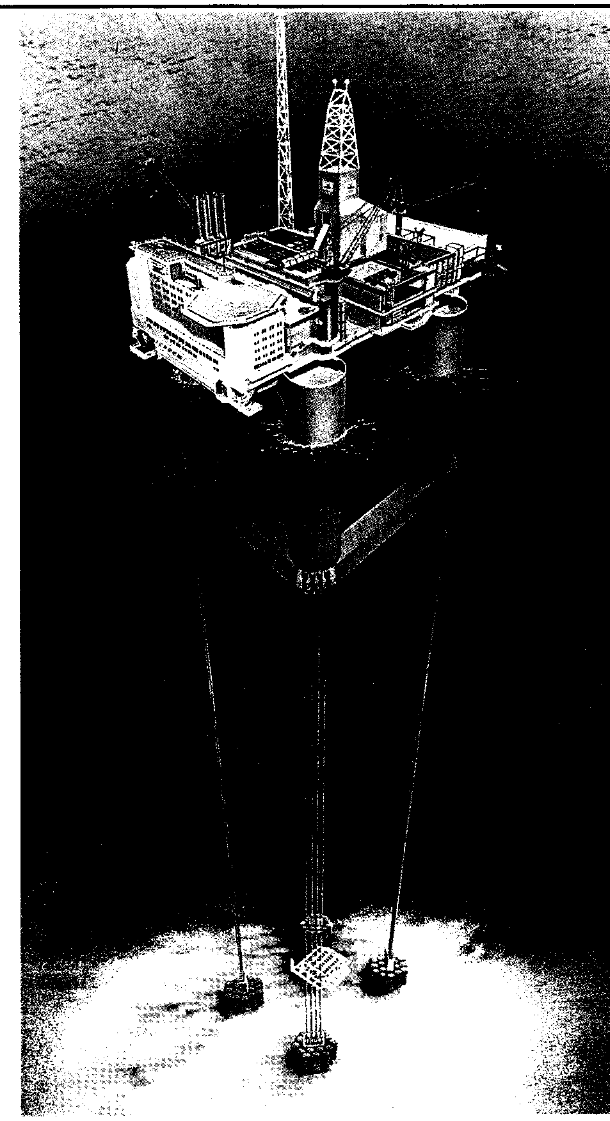

Figure 6. The Heidrun tension leg platform.

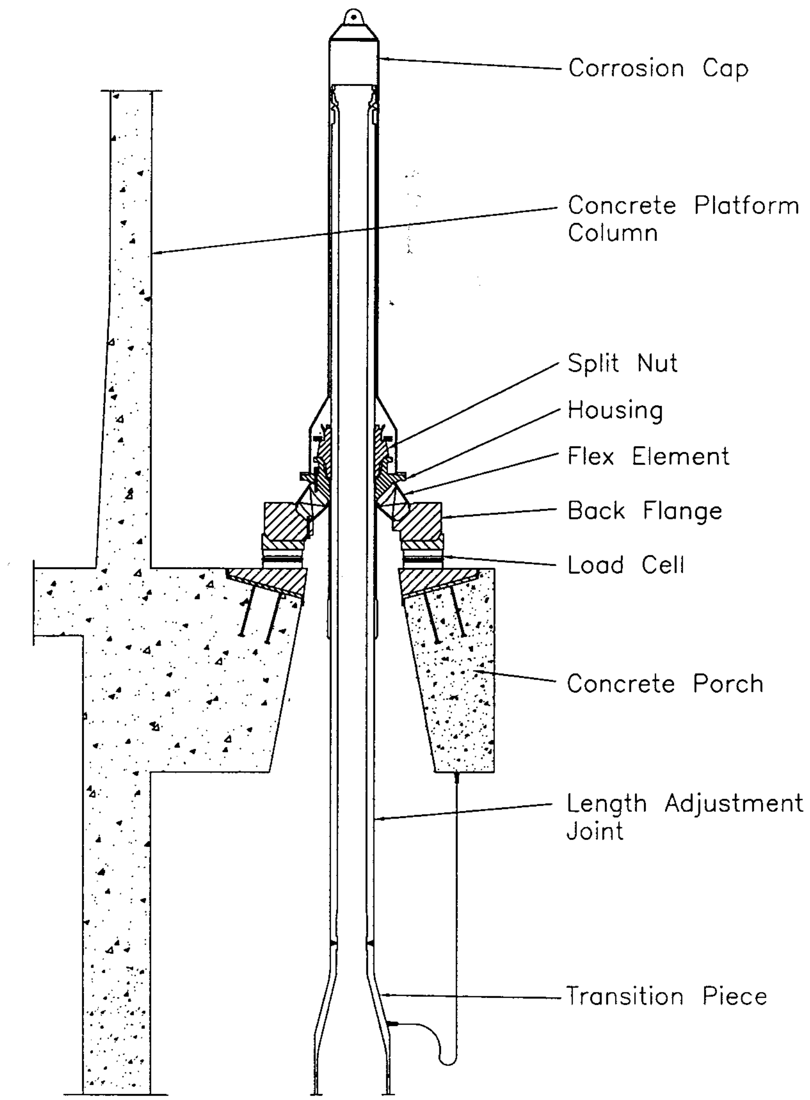

Figure 7. The components of the tendon top connector assembly.

and iterative solutions in structural analyses. We see that the solution time and also required disk storage can be very much smaller. However, the actual savings depend on the specific coefficient matrix considered. If the matrix is not well-conditioned, such as typically encountered in the analysis of shell structures, the solution time using the iterative solver may only be little less or even larger than when using the direct solver. However, storage is saved in practically all cases when a large set of equations is solved.

4.2. Analysis of Top Connector for a Tension Leg Platform

Finite element analyses play a major role in the integrated design of critical parts of offshore-structures. Figure 6 shows the Heidrun tension leg platform, which is

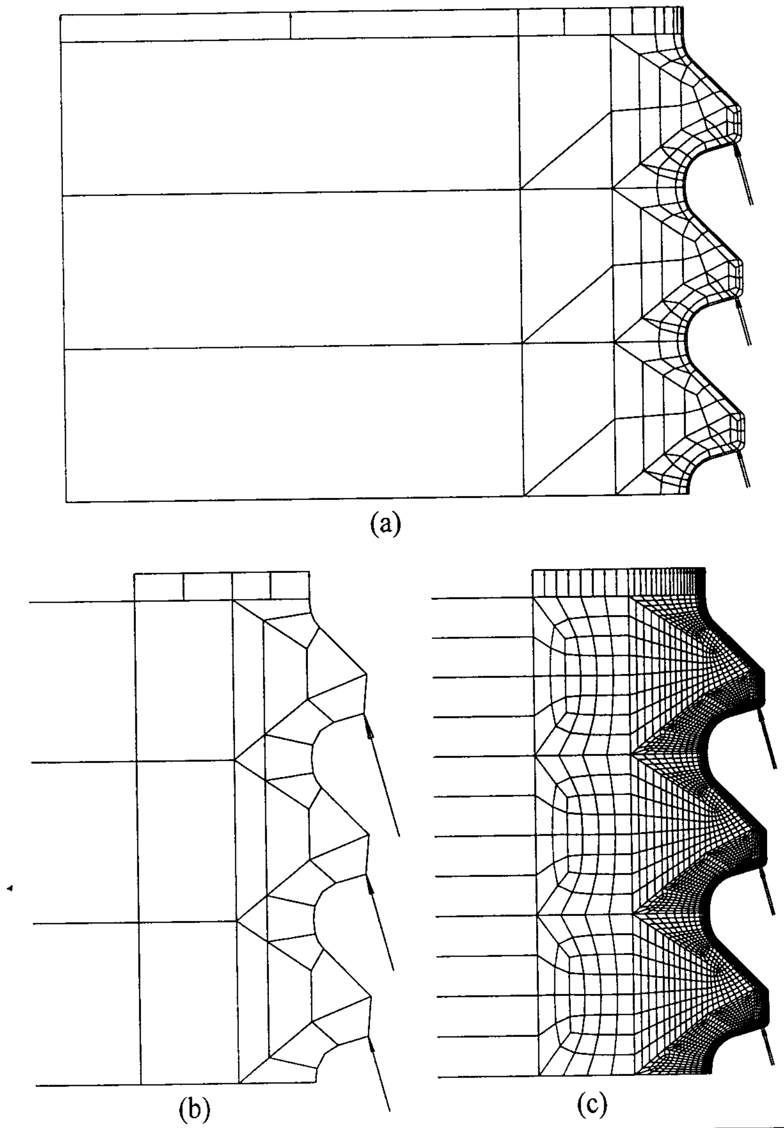

Figure 8. Some finite element models used in the axisymmetric analysis convergence study.

the first tension leg platform with a concrete hull and the largest tension leg platform ever built, incorporating one of the world's largest offshore modules. The great importance of an adequate finite element analysis of this structure is apparent because of the 1993 failure of the Sleipner platform, partly due to an inadequate finite element analysis (not performed using ADINA). This failure led to huge losses.

Here, we briefly refer to some finite element analyses of the tendon top connector assembly published by Bøyum (1995), see Figures 7 to 12. The top connector assembly is a critical part, demanding high strength within limited weight and dimensions. Because of the importance of this structural component, a detailed analysis was performed, which included mesh convergence studies.

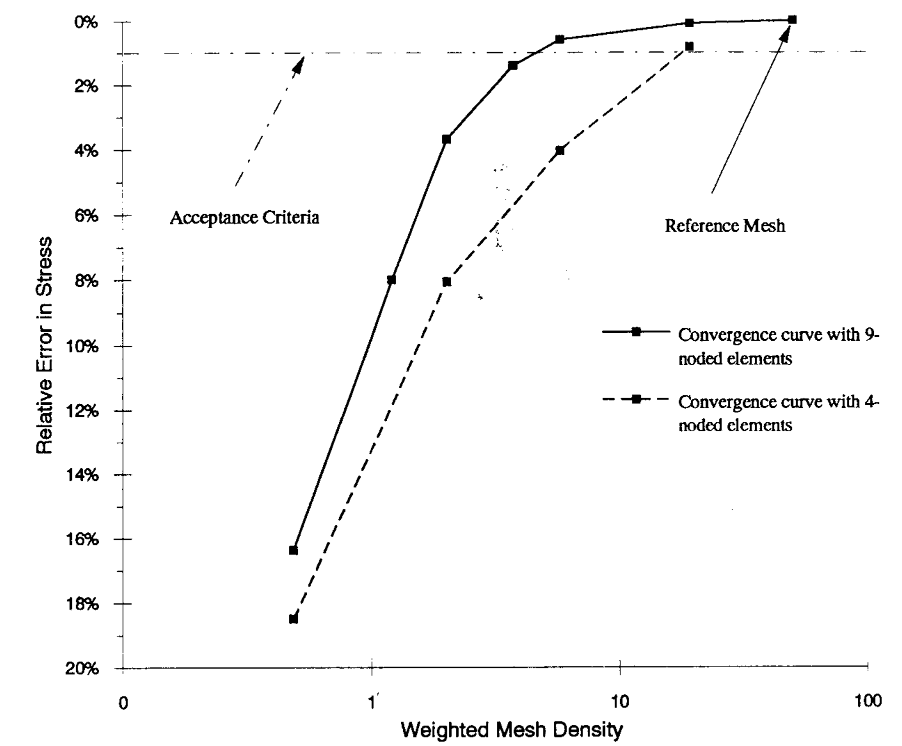

Figure 9. Results of convergence study (the reference mesh is mesh (c) in Fig. 8).

Large finite element systems had to be solved, including contact conditions in the threaded sections and effects of plasticity. The iterative solver, also used for the solutions in Figures 3 to 5, and the contact algorithm in ADINA were important assets in the complete analysis process, see Figure 12. For such major and costly structures, it is clear that state-of-the-art tools should be employed in the analysis.

4.3. Seismic Analysis of California Major Bridges, Including the San Francisco to Oakland Bay Bridge

After the recent earthquakes in California, the State of California decided to review the major bridges for their seismic safety and the need for retroactive strengthening. It was stipulated that for this very important and large project, state-of-the-art analysis tools should be employed, and the ADINA program was selected to be used in all phases of the analyses. Seven major bridges are currently being analyzed, including the well-known Bay Bridge from San Francisco to the Oakland/Berkeley area (see Figures 13-14).

The finite element idealizations represent state-of-the-art models of the bridges. In some analyses, the complete bridges are represented globally and subjected to earthquake loadings of 10 and more seconds. These representations are based largely on beam elements and include nonlinear large displacement effects, material nonlinearities, and contact conditions within the bridges and the support environments. In other analyses, details of the bridges are being

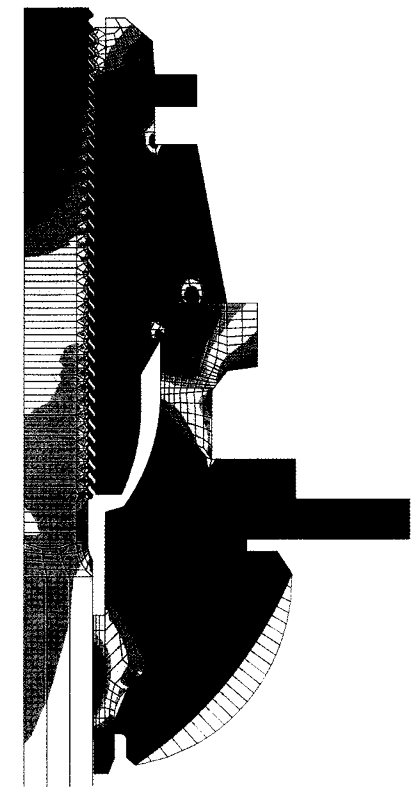

Figure 10. Deformed mesh of tendon top connector assembly, axisymmetric model under extreme load.

analyzed, in which for example, accurate shell models are used to represent member connections.

A typical model of a section of the Bay Bridge is shown in Figure 15.

The bridge analyses are carried out by the California Department of Transportation and contractors. The simulations to identify the collapse capacities of the bridges are the corner-stone for the retroactive strengthening of members and connections in the bridges. This strengthening will result in less destruction and an increase in the public safety in the event of a severe earthquake.

4.4. Analysis of Missile Launch Device

Simulations of structures and fluids have been used extensively in the defense industries. Figure 16 shows the finite element representation of a launching device for a missile. The model of the missile itself is also shown, but better seen in Figure 17.

The steel tube guides the missile after firing and is subjected to very high stresses. The objective of the analysis is to simulate the launching process for an assessment of the stresses in the tube. The analysis requires the simulation of the sliding and bouncing of the missile within the tube while the tube vibrates during launch.

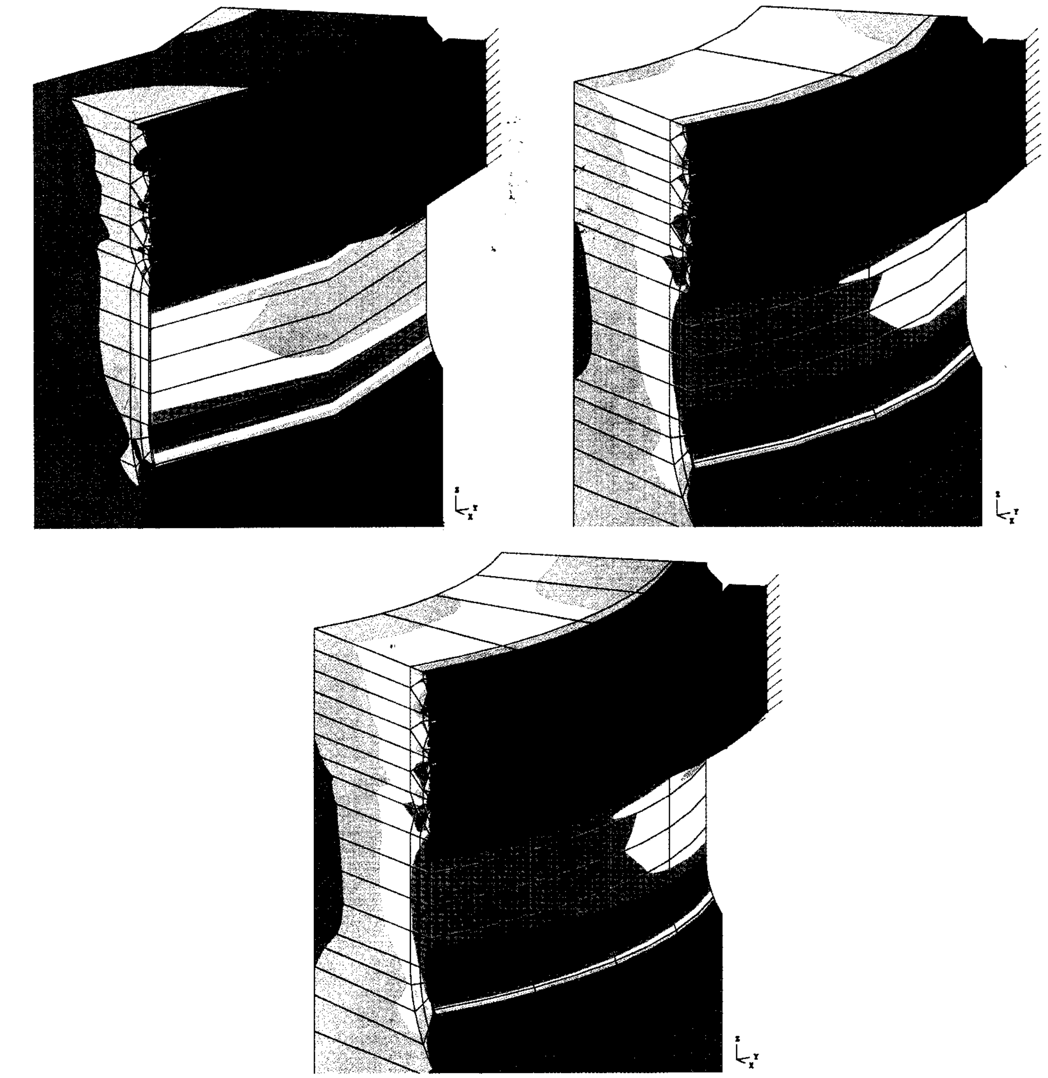

Figure 11. Parts of three-dimensional models used in convergence tests.

Figures 16 and 17 show the initial position of the missile and its position upon leaving the tube. Figure 18 shows some deformations in the tube during the launching process.

4.5. CFD Analysis of Heat Transfer in a Washer-Drier Channel

There are obviously numerous physical problems in the design of appliances where the simulation of fluid flow including heat transfer can be very valuable. The prediction of the fluid flow and heat transfer can be a great asset in reaching an effective design.

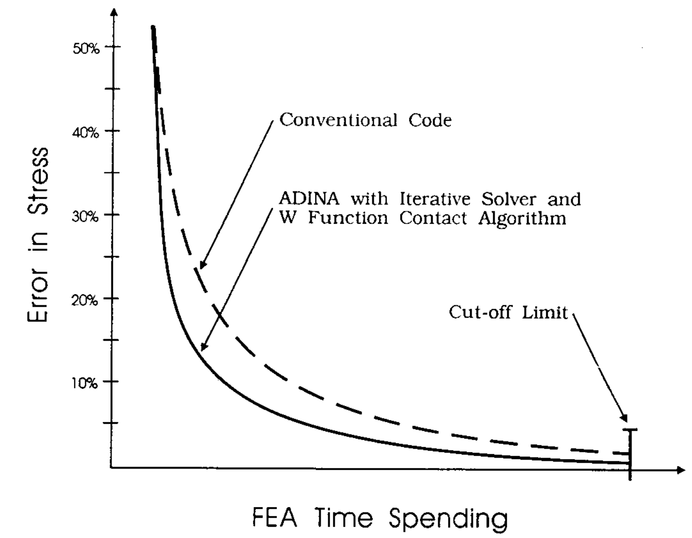

Figure 12. Correlation between error in stress and solution time.

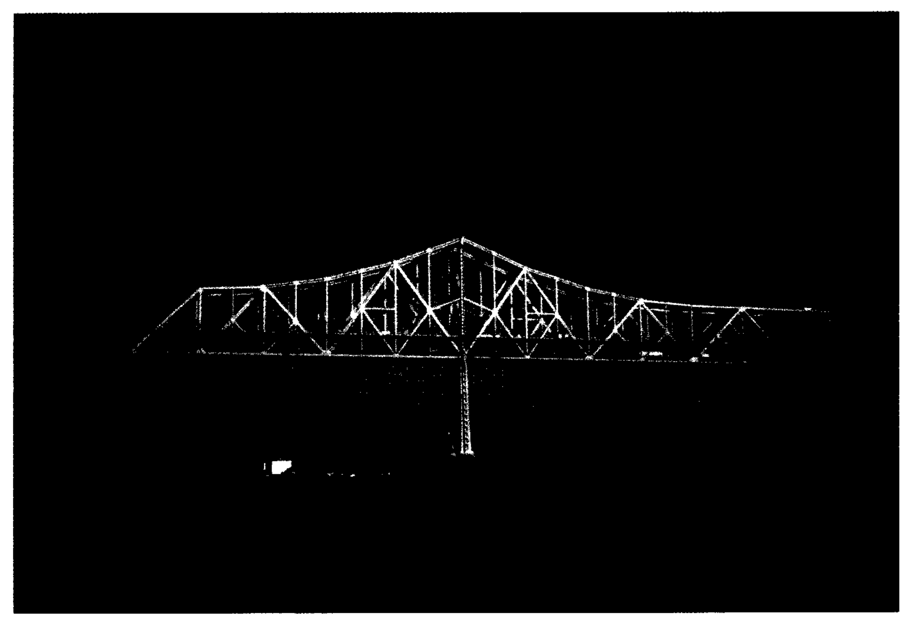

Figure 13. Part of San Francisco-Oakland Bay Bridge: General picture.

Here, we mention the results obtained by Reimers, Scheider, and Schneider (1995) in the CFD analysis of a washer-drier heating channel. Figures 19 and 20 show the washer-drier and the heating channel. The air inside the drier is sucked out, enters a condenser, and flows through the heating channel for reheating. The objective of the analysis was to predict the air velocity profiles and the temperature distribution within the channel and its housing. The analysis was performed using

Figure 14. San Francisco-Oakland Bay Bridge: Failure of top slab in the 1989 earthquake.

the incompressible fluid flow model including turbulence effects, see Section 2.2, and a conjugate heat transfer capability (see the ADINA system users manuals, 1995).

Figures 21 and 22 show the finite element discretization used to represent the air and heating channel and some velocity and temperature results. For more details, we refer the reader to Reimers et al. (1995).

4.6. Analysis of Fluid Flow Valve

Figure 23 shows schematically the valve analyzed. The difficulty in this analysis is that the structure is very thin and loaded with a relatively large pressure. The gas flow within the valve prevents complete closure, however, the gap of initial width 0.007 in. is considerably decreased. Hence, the Lagrangian formulation was used for the structure and the arbitrary Lagrangian-Eulerian formulation for the fluid modeled as a compressible medium (see Sections 2.3 and 2.4). Planar conditions were assumed.

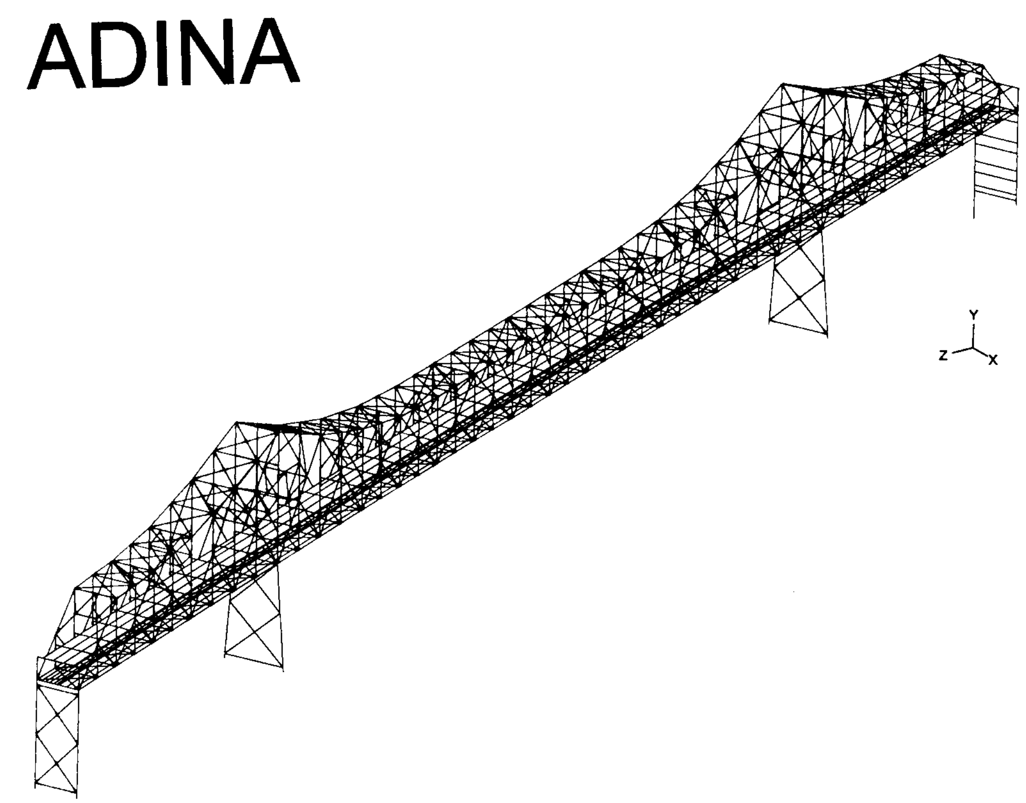

Figure 15. Model of section of Bay Bridge.

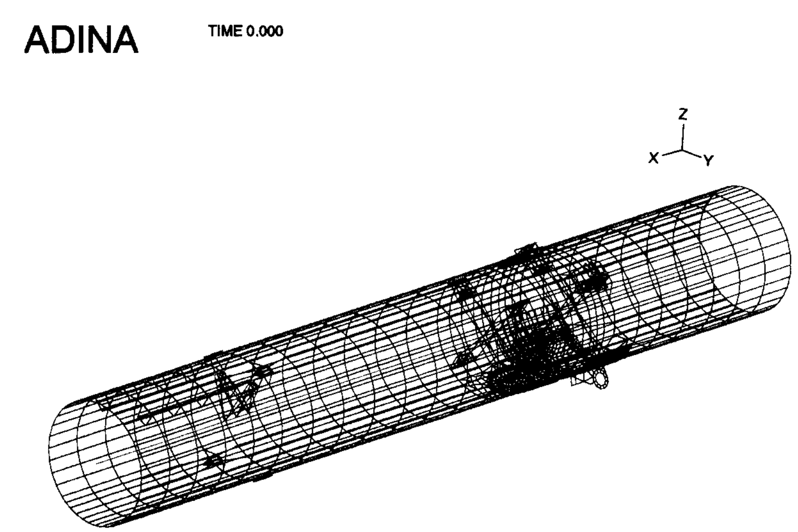

Figure 16. Finite element model of missile launching tube with missile in initial position.

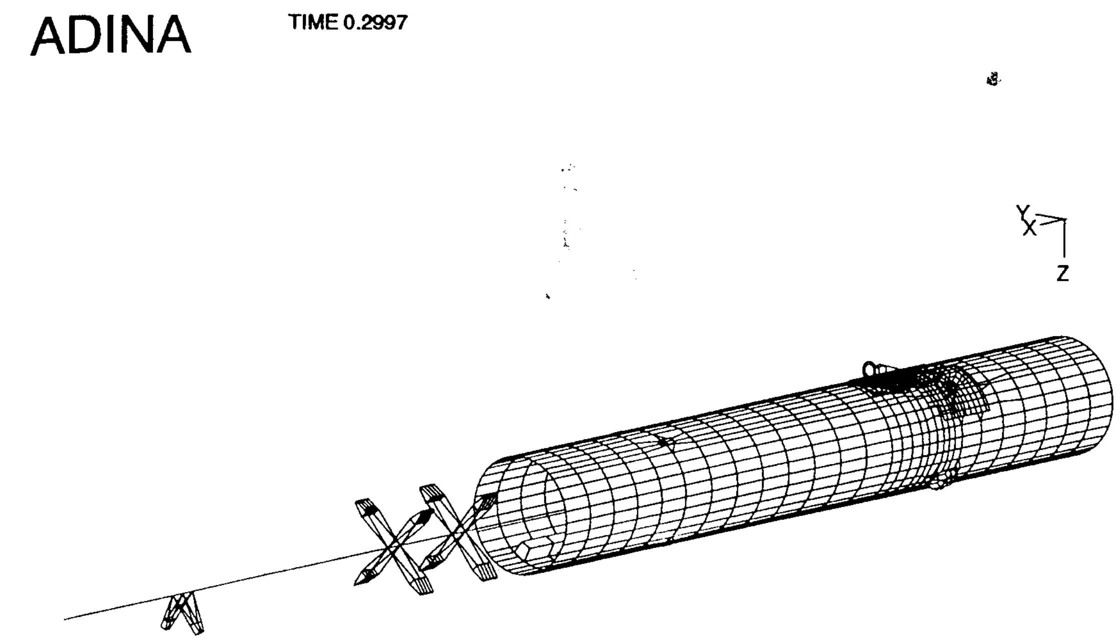

Figure 17. Missile leaving launching tube.

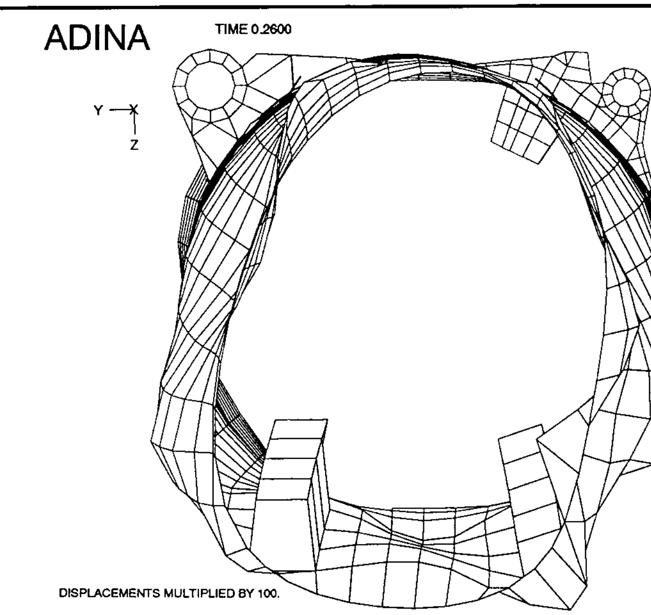

Figure 18. Typical deformations of tube during missile launch.

Figures 24 and 25 show some details of the finite element model used and some solution results. The analysis, performed in a few hours on an engineering workstation, illustrates the complexities of solutions in fluid-structure interac-

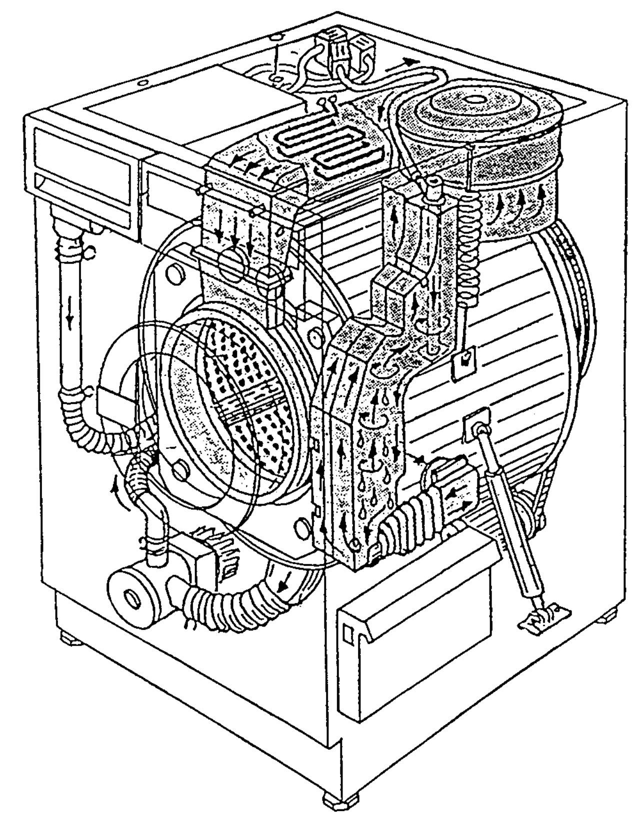

Figure 19. Illustration of washer-drier.

tions that are currently sought. A fully three-dimensional analysis of this kind, although possible, will of course require considerable computing resources.

5. CONCLUDING REMARKS

The objective in this article was to survey some current state-of-the-art analysis approaches and present appropriate illustrations. Although very complex analyses can already be performed, important further developments are in need. We want to mention the following important research and development tasks.

The automatization of finite element analysis in computer-aided design is a most important development. The need is not only to automatize the finite element solution of the chosen mathematical model, but to develop algorithms that, in the first instance, help the designer to choose an appropriate mathematical model. These procedures therefore should also change or refine the mathematical model when necessary (depending on the questions asked by the analyst). Because there is clearly a close coupling between the optimization of a design and the mathematical model chosen for analysis, the algorithms should also address the issues arising in the optimization. Of course, some developments have taken place in

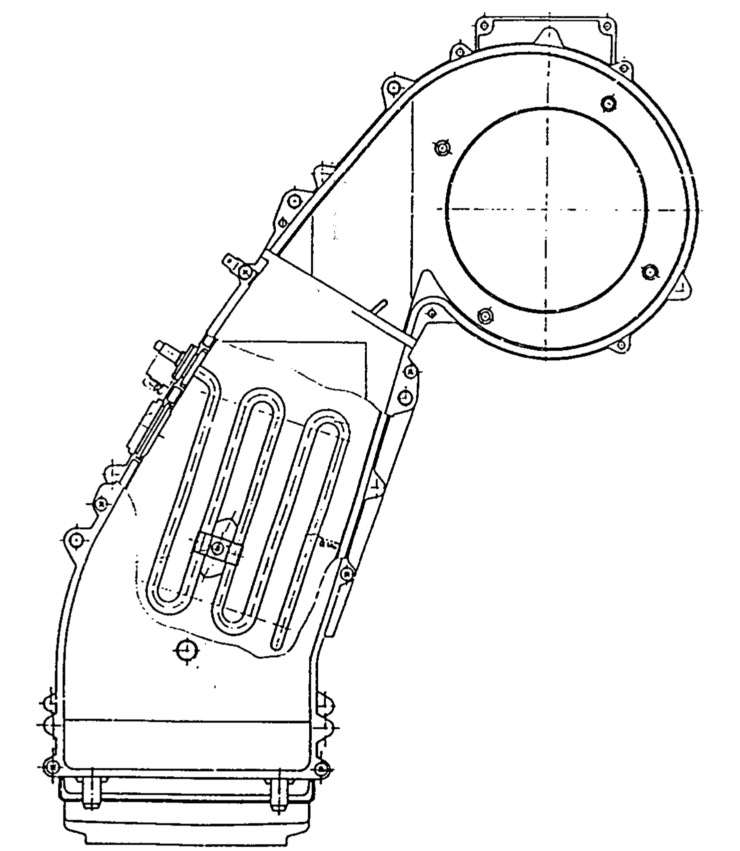

Figure 20. Design drawing of heating channel.

these areas, but general and efficient algorithms for the *integrated* process of choosing the appropriate mathematical model, the automatic solution of the model (see Figure 1) and the optimization of the design are still far from being available.

Considering nonlinear analysis, developments in many areas are still needed. These include improvements in the nonlinear algorithms for contact problems, physical instabilities, coupled physical situations, materially highly nonlinear problems, three-dimensional damage and fracture, high Reynolds and Peclet number flows, turbulent flows, and fluid flows with structural interactions.

Finally, there will be a continuous need to solve larger and larger finite element systems. This need is driven by the requirement to solve ever more complex structural and fluid flow problems. The accurate simulation of these problems will be helped by increasingly more powerful iterative solution schemes and by the use of parallel processing techniques. We mentioned earlier the importance of iterative solution techniques, but also want to emphasize that the efficient use of shared memory and distributed memory parallel processing hardware/software environments should result in very much enhanced programs for very large finite element systems.

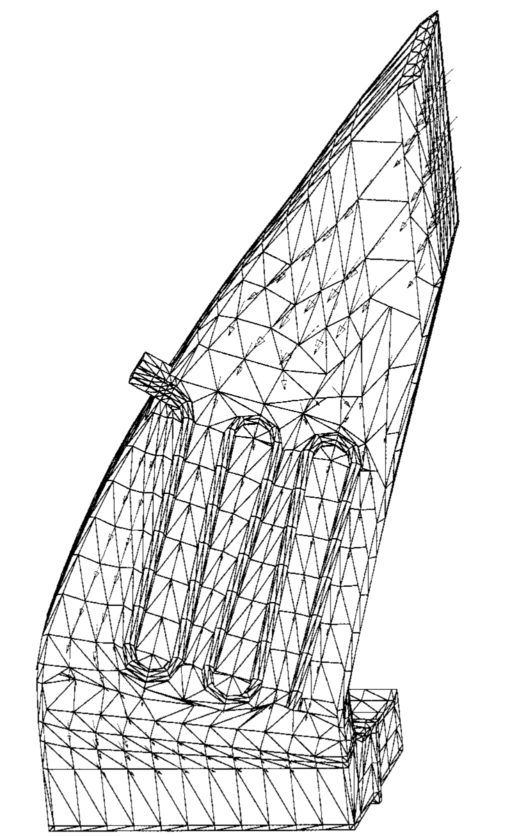

Figure 21. Some velocity results of analysis of heating channel. (The mesh used is also shown.)

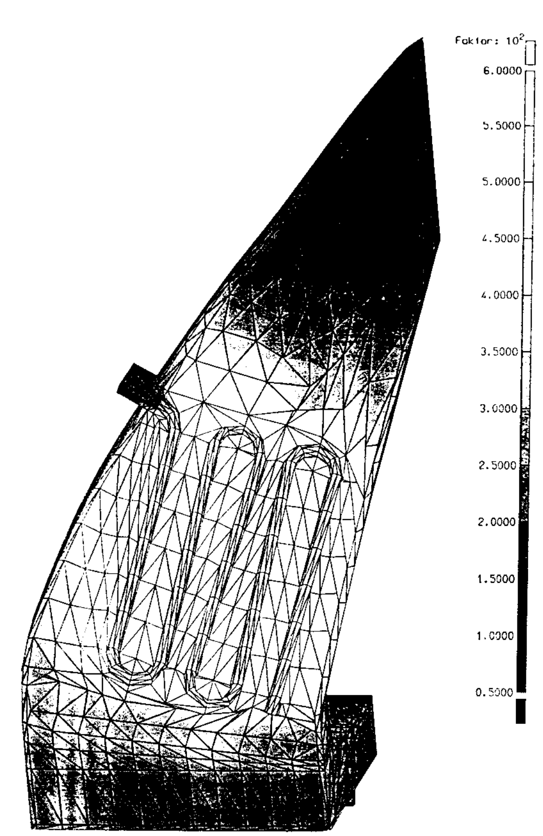

Figure 22. Some temperature results of analysis of heating channel.

REFERENCES

The ADINA system users manuals, 1995, ADINA R & D, Inc., 71 Elton Avenue, Watertown, MA 02172.

Bathe, K. J., 1995, *Finite Element Procedures*, Prentice Hall, Englewood Cliffs, NJ.

Bathe, K. J., Bucalem, M., and Brezzi, F., 1990, "Displacement and stress convergence of our MITC plate bending elements," *Journal of Engineering Computations* **7**, 291-302.

Bathe, K. J. and Dvorkin, E. N. 1986, "A formulation of general shell elements—The use of mixed interpolation of tensorial components," *International Journal for Numerical Methods in Engineering* **22**, 697-722.

Bathe, K. J., Lee, N. S., and Bucalem, M., 1990, "On the use of hierarchical models in engineering analysis," *Computer Methods in Applied Mechanics and Engineering* **82**, 5-26.

Bathe, K. J., Nitikitpaiboon, C., and Wang, X., 1995, "A mixed displacement-based finite element formulation for acoustic fluid-structure interaction," *Journal of Computers and Structures* **56**, 225-237.

Bathe, K. J., Walczak, J., and Zhang, H., 1993, "Some recent advances for practical finite element analysis," *Journal of Computers and Structures* **47**, 511-521.

Bathe, K. J., Zhang, H., and Wang, M. H., 1995, "Finite element analysis of incompressible and compressible fluid flows with free surfaces and structural interactions," *Journal of Computers and Structures* **56**, 193-214.

Blacker, T. D. and Meyers, R. J., 1993, "Seams and wedges in plastering: A 3-D hexahedral mesh generation algorithm," *Engineering with Computers* **9**, 83-93.

Bøyum, E., 1995, "Analyses of top connectors for a TLP using ADINA," *Journal of Computers and Structures* **56**, 269-281.

Brezzi, F. and Bathe, K. J., 1990, "A discourse on the stability conditions for mixed finite element formulations," *Computer Methods in Applied Mechanics and Engineering* **82**, 27-57.

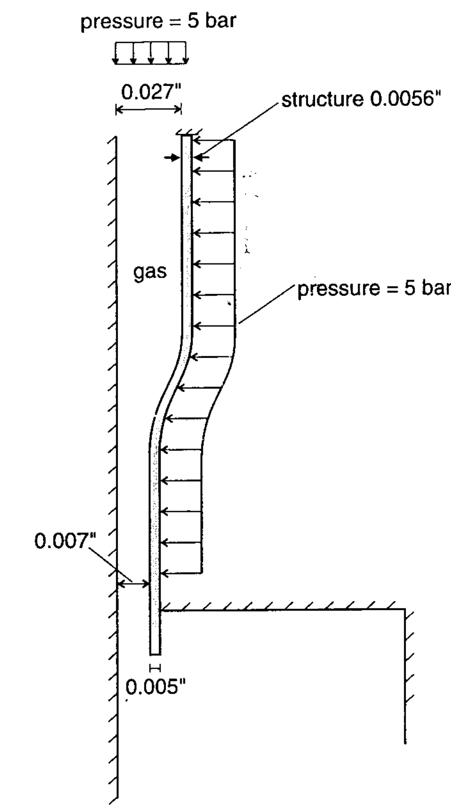

Figure 23. Schematic of fluid flow valve.

Bucalem, M. L. and Bathe, K. J., 1993, "Higher-order MITC general shell elements," *International Journal for Numerical Methods in Engineering* **36**, 3729-3754.

Franca, L. P., Frey, S. L., and Hughes, T.J. R., 1992, "Stabilized finite element methods: I. Application to the advective-diffusive model," *Computer Methods in Applied Mechanics and Engineering* **95**, 221-242.

Gabriel, G. and Bathe, K. J., 1995, "Some computational issues in large strain elasto-plastic analysis," *Journal of Computers and Structures* **56**, 249-267.

George, P. L., 1991, *Automatic Mesh Generation*, Wiley, New York.

Lee, N. S. and Bathe, K. J., 1994, "Error indicators and adaptive remeshing in large deformation finite element analysis," *Finite Elements in Analysis and Design* **16**, 99-139.

Lewis, R. L. and Schrefler, B. A., 1987, *The Finite Element Method in the Deformation and Consolidation of Porous Media*, Wiley, New York.

Patankar, S. V., 1980, *Numerical Heat Transfer and Fluid Flow*, Hemisphere, Bristol, PA.

Reimers, P., Scheider, I., and Schneider, A., 1995, "CFD analysis of conjugate heat transfer in a washer-drier heating channel," *Journal of Computers and Structures* **56**, 215-223.

Sussman, T. and Bathe, K. J., 1986, "Studies of finite element procedures—Stress band plots and the evaluation of finite element meshes," *Journal of Engineering Computations* **3**, 178-191.

Sussman, T. and Bathe, K. J., 1987, "A finite element formulation for nonlinear incompressible elastic and inelastic analysis," *Journal of Computers and Structures* **26**, 357-409.

Wang, X. and Bathe, K. J., 1995, "Displacement/pressure based mixed finite element formulations for acoustic/slosh fluid-structure interaction problems," submitted for publication.

Zienkiewicz, O.C. and Taylor, R. L., 1989/1990, *The Finite Element Method, Vols. 1 and 2*, (4th ed.). McGraw-Hill, New York.

Zienkiewicz, O. C. and Zhu, J.Z., 1987, "A simple error estimator and adaptive procedure for practical engineering analysis," *International Journal for Numerical Methods in Engineering* **24**, 337-357.

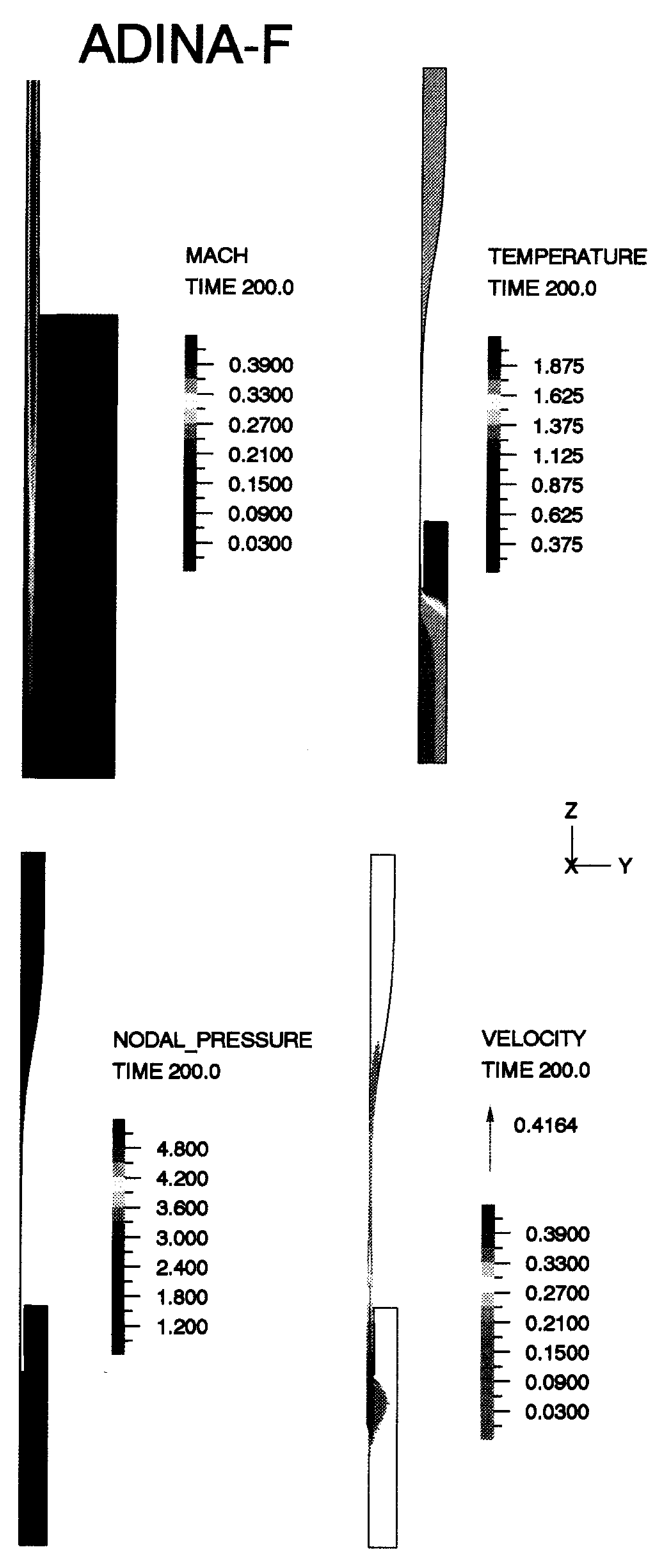

Figure 24. Some results of analysis of valve.

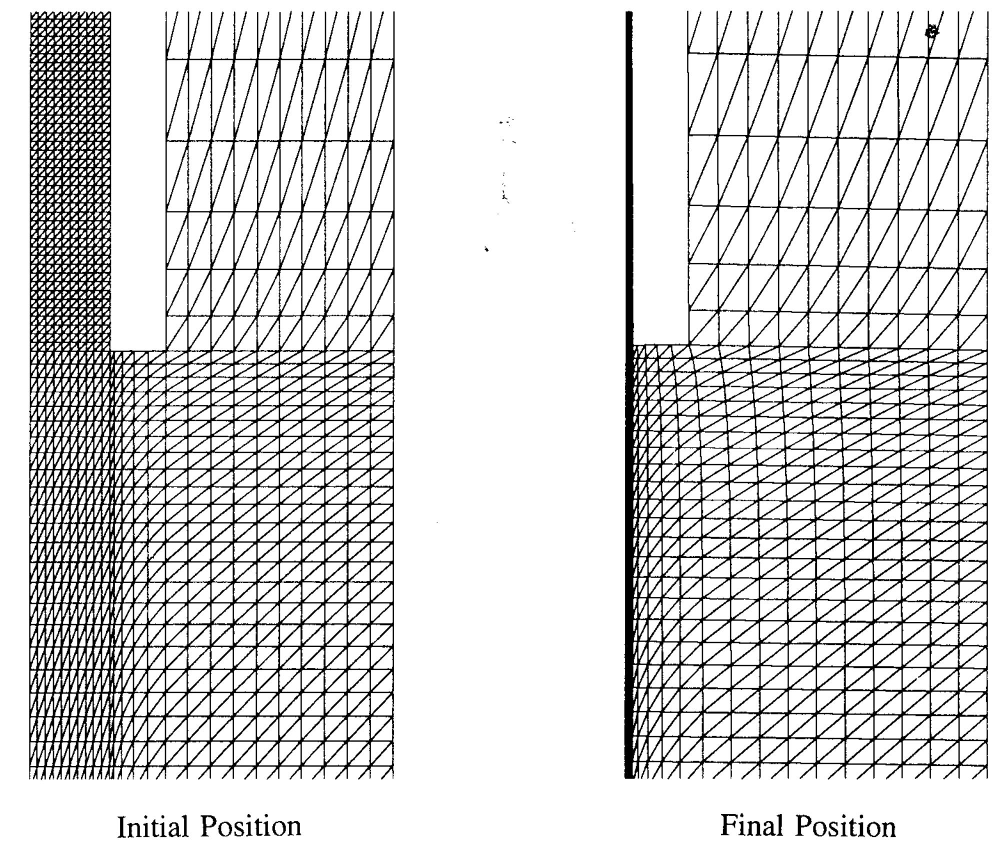

Figure 25. Analysis of valve: Fluid mesh at tip of structure, initial and final positions.